Published in final edited form as:
Chem Sci. 2013 ; 4(5): 2122–2126. doi:10.1039/C3SC50252J.

Poly(ethylene oxide)-*block*-polyphosphester-based Paclitaxel Conjugates as a Platform for Ultra-high Paclitaxel-loaded Multifunctional Nanoparticles†

Shiyi Zhang[a,b,‡], **Jiong Zou**[a,‡], **Mahmoud Elsabahy**[a,c], **Amolkumar Karwa**[d], **Ang Li**[a,e], **Dennis A. Moore**[d], **Richard B. Dorshow**[d,f], and **Karen L. Wooley**[a,*]

[a]Departments of Chemistry and Chemical Engineering, Laboratory for Synthetic-Biologic Interactions, Texas A&M University, P.O. BOX 30012, 3255 TAMU, College Station, TX 77842, USA

[b]Department of Chemistry, Washington University in St. Louis, St. Louis, MO 63130, USA

[c]Department of Pharmaceutics, Faculty of Pharmacy, Assiut University, Assiut, Egypt

[d]Covidien Pharmaceuticals R&D, Hazelwood, MO 63042, USA

[e]Al-Deera Holding USA, Inc., New York, NY 10019

[f]MediBeacon, Inc., St. Louis, MO 63146, USA

Abstract

A new type of degradable, nanoscopic polymer assembly containing ultra-high levels of drug loading *via* covalent attachment within amphiphilic core-shell nanoparticle morphology has been generated as a potentially effective and safe anti-cancer agent. Poly(ethylene oxide)-*block*-polyphosphoester-based paclitaxel drug conjugates (PEO-*b*-PPE-*g*-PTX) were synthesized by rapid, scalable and versatile approach that involves only two steps: organocatalyst-promoted ring-opening-polymerization followed by click reaction-based conjugation of a PTX prodrug. Variations in the polymer-to-PTX stoichiometries allowed for optimization of the conjugation efficiency, the PTX drug loading and the resulting water solubilities of the entire polymer and the PTX content. The PEO-*b*-PPE-*g*-PTX formed well-defined micelles in aqueous solution, with a PTX loading capacity as high as 65 *wt*%, and a maximum PTX concentration of 6.2 mg/mL in water, which is 25000-fold higher than the aqueous solubility of free PTX. The positive cell-killing activity of PEO-*b*-PPE-*g*-PTX against several cancer cell lines is demonstrated, and the presence of pendant reactive functionality provides a powerful platform for future work to involve conjugation of multiple drugs and imaging agents to achieve chemotherapy and bioimaging.

Paclitaxel (PTX), a microtubule-interfering agent, has demonstrated a broad spectrum of antitumor activity against various cancers including breast, lung and advanced ovarian

†Electronic Supplementary Information (ESI) available: [detailed experimental section, including data from studies of polymer chemical modification, solubility, degradation and cell internalization]. See DOI: 10.1039/b000000x/

Tel. (979) 845-4077, wooley@chem.tamu.edu.
‡These authors contributed equally to this work.

cancers,[1, 2] however, there are several challenges with its formulation that remain unmet. The low solubility of PTX and the difficulty of achieving sufficiently high concentration in solution that is suitable for *in vivo* administration and clinical applications have led to the development of various strategies to increase its bioavailability, which utilize low molecular weight surfactants (Taxol®),[3] coat the drug with albumin (Abraxane®),[4] or conjugate it to water-soluble polymers (PTX poliglumex, OPAXIO™, CT-2103, Xyotax®).[5] Toxicity and hypersensitivity reactions associated with the vehicles (*e.g.* Cremophor-EL, polyethoxylated castor oil) and the non-selectivity of these formulations calls for the development of degradable nanoparticle carriers that can achieve high loading of the drug, exhibit low toxicity, are capable of extended circulation *in vivo*, and have a possibility of versatile chemical modifications, for instance, for conjugation of imaging agents and targeting ligands.[6, 7] Poly-(L)-glutamic acid (PGA) offers carboxylic acid side chain substituents for conjugation of PTX and other moieties, and PGA-PTX conjugates have entered clinical evaluation under the brand name OPAXIO™. Although PGA-PTX gave significantly enhanced water solubility and antitumor activity, with lower toxicity, than the free drug in preclinical studies,[5, 8–10] conjugation of the 2'-hydroxyl of PTX by ester linkage to the γ-carboxylic acid side chains of PGA proceeds without control over the placement of the PTX along the backbone of the polymer, resulting in ill-defined multi-molecular aggregates. With the statistical distribution of PTX along the PGA chain, only relatively low loadings could be tolerated, 37 *wt*% PTX loading by weight, to maintain dispersibility of the PGA-PTX, which provides a maximum PTX concentration in water of 2.6 mg/mL.[9] A number of degradable and non-degradable drug conjugate systems[11] have been used as components of medical devices in PTX delivery, for instance, PTX-conjugated polyvalent DNA-functionalized gold nanoparticles,[12] polylactide(PLA)-PTX conjugated nanoparticles[13] and PTX cross-linked PLA based nanocomposites.[14] It still remains challenging to obtain high PTX loadings for polymer drug conjugates (PDCs) and also maintain high water solubility to be suitable for *in vivo* administration and clinical applications. Therefore, we have taken advantage of current state-of-the-art synthetic polymer chemistry and orthogonal conjugation chemistries[15, 16] to produce, through a rapid, versatile and scalable two-step approach, unique degradable diblock copolymers of poly(ethylene oxide) and functional polyphosphoesters that allow for click conjugation of PTX onto a selective region of the amphiphilic diblock copolymer, thereby, allowing ultra-high PTX loading within nanoscopic carriers in water.

Based upon an interest to incorporate a non-reactive, water-soluble polymer chain segment, to mediate the supramolecular assembly process in water and provide a shell layer that imparts serum stability, together with a highly- and selectively-reactive chain segment for high-loading conjugation of PTX, a new type of poly(ethylene oxide)-*b*-polyphosphoester (PEO-*b*-PPE)-based polymer drug conjugate for PTX delivery was designed. Surface modification of nanoparticles with PEO moieties have the benefits of prolonged blood circulation and enhanced accumulation in the tumor tissues *via* the enhanced permeability and retention (EPR) effect.[17] The PPE portion of the system was constructed based upon our recent development of a new type of degradable and water-soluble polyphosphoester bearing alkynyl functionalities by using organocatalyst-promoted ring opening polymerization (ROP).[18, 19] The alkynyl groups on the side chain have been shown to undergo high-

efficiency reactions in “click”-type azide-alkyne Huisgen cycloaddition. Therefore, an azide-functionalized PTX was synthesized by esterification, in which the most reactive 2'-hydroxyl group of PTX reacted with 6-azidohexanoic acid to form an ester linkage, and then this azide-functionalized PTX was further conjugated onto the PPE backbone through click reaction, resulting in PEO-*b*-PPE-*g*-PTX drug conjugates that assembled in water into nanoscopic micelles with up to 65 *wt*% PTX loading. To our best knowledge, this drug loading capacity is the highest, compared to the reported polymer-PTX conjugates. The high content of PTX in the drug conjugates is important to increase potency, decrease the total amount of polymers required to deliver a particular amount of the drug, and reduce any potential toxicities that might be associated with the delivery vehicle. Taking advantage of the high solubility of the PPE backbone and the PEO shielding, the solubility of PTX could reach 6.2 mg/mL. The potency of the resulting PEO-*b*-PPE-*g*-PTX drug conjugates was also tested against multiple cancer cell lines. Though PEO-*b*-PPE-*g*-PTX micelles were one-to-two orders of magnitude less potent than free PTX, their cell killing ability was better than or equal to the performance of PGA-PTX. Residual alkynyl groups were decorated with fluorescent dyes to track the cellular uptake of the PEO-*b*-PPE-*g*-PTX conjugates *in vitro*.

The PEO-*b*-(PPE-*g*-PTX) conjugates were synthesized as illustrated in Figure 1. PEO (average M_n ~2,000 Da) (**1**) was used to initiate the ROP of butynyl phospholane (BYP), **2**, which yielded the well-defined diblock copolymer, PEO_{44}-*b*-$PBYP_{30}$, **3**. This controlled organocatalyzed ROP of the cyclic phospholane monomer gave quantitative conversion in only 4 min, and was highly reproducible. With a 1:30 stoichiometry of PEO:BYP, **3** was produced having M_n = 7200 Da, in agreement with the theoretical degrees of polymerization, as determined by ^{1}H NMR spectroscopy, and narrow molecular weight distribution, M_w/M_n = 1.17, as determined by gel permeation chromatography (GPC) (for full characterization data, see supporting information).

To equip PTX with a functionality for coupling to PEO-*b*-PPE, the C-2'-OH position of PTX was functionalized with an azido group through an ester linkage, by reaction with 6-azidohexanoic acid and employing a slight excess of PTX (1.2 eq), in the presence of *N,N'*-dicyclohexylcarbodiimide and 4-(dimethylamino)pyridine in CH_2Cl_2 heated at reflux for 3 d to afford PTX C2'-ester **4** as the predominant product. Automated high performance flash chromatography with prepacked fine spherical silica gel (20–40 μm) was used to isolate **4** in 78% yield. According to the literature, by using DCC/DMAP promoted condensation, only the 2’-OH of PTX is active.[20] The selective condensation between 2’-OH and 6-azidohexanoic acid was confirmed by ^{1}H NMR spectroscopy. The 2’(C<u>H</u>)-OH on PTX in $CDCl_3$ resonates at 4.78 ppm. In the ^{1}H NMR of azido-PTX, no peak was observed between 4.6–4.9 ppm (see supporting information). In contrast, no significant chemical shift change was observed for the (C-7)-C<u>H</u>-OH signal (at 4.40 ppm) before and after esterification.

Azide-alkyne Huisgen cycloaddition (CuAAC) was employed to attach **4** onto the backbone of **3** and afford PEO-*b*-(PPE-*g*-PTX), **5**. PEO-*b*-(PPE-*g*-PTX) conjugates were synthesized with a range of feed ratios of azido-PTX to PEO-*b*-PPE alkyne (20%, 50% and 100%). As shown in Figure S1, even though the conjugation efficiency decreased as the feed ratio increased, the click reaction showed higher conjugation efficiency than that observed for esterification-based conjugation of sterically-bulky PTX onto polymers.[14, 21, 22] The highest

PTX loading capacity, 65 wt%, was reached when the feed ratio was 100%, however, this polymer had a poor solubility in water (lower than 0.5 mg/mL). The optimal polymer had conjugation efficiency as high as 90%, PTX loading capacity of 55 wt%, and high water solubility (11.3 mg/mL) when the feeding ratio of **4** to **3** was 15 to 1 (feed ratio of azido-PTX to alkyne was 50%). Unreacted **4** was removed by repeated precipitation from acetone into diethyl ether 3 times, because PTX and azido-PTX were well soluble in diethyl ether. Complete removal of the unreacted **4** was confirmed by ^{1}H NMR, GPC and HPLC (Figure S2 shows the comparison of **5** and PTX) analysis of the product.

The PEO-*b*-(PPE-*g*-PTX) drug conjugates, **5**, were further purified and supramolecularly assembled in water by being dissolved in acetone and dialyzed against nanopure water containing Chelex 100 resin (100–200 mesh) for 2 d, to remove copper and other potential ion contaminants, and also to trigger self assembly. The resulting micelle solution was obtained and then passed through a 450 nm polypropylene filter to remove dust and large aggregates. The micelle solution was lyophilized to give a faint yellow powder with an overall yield above 90%. The lyophilized PEO-*b*-(PPE-*g*-PTX) conjugates could be easily dissolved into water at a concentration as high as 11.3 mg/mL (equivalent PTX concentration of 6.2 mg/mL) by applying sonication for 3 min (see supporting information for the solubility test). Dynamic light scattering (DLS) analysis indicated the number-average hydrodynamic diameter of the micelles was 26 ± 7 nm, and transmission electron microscopy (TEM) images confirmed that the PEO-*b*-(PPE-*g*-PTX) nanoassemblies were well-dispersed in water in the form of micellar nanoparticles with a narrow size distribution D_{av} = 24 ± 6 nm (Figure 2).

Click reactions have been shown to be highly efficient when coupling large-sized anticancer drugs.[20, 23, 24] Here, click chemistry provided a highly-efficient strategy to load PTX onto reactive polymer backbones in high coupling conversion and PTX loading capacity. PEO-*b*-(PPE-*g*-PTX) drug conjugates, **5**, were dissolved in water at the equivalent PTX concentration of 6.2 mg/mL, exhibiting significantly enhanced solubility, *ca*. 25,000-fold, as compared to the free drug, and 2.4-fold higher than that reported for the PTX conjugates with PGA.[9]

The lyophilized, powder-like PEO-*b*-(PPE-*g*-PTX) conjugates showed no evidence of degradation of structure or properties over 3 months when stored under nitrogen at −20°C. The GPC profile and DLS analysis confirmed that the chemical compositions of the polymer-drug conjugates and the particle sizes of the micelles did not change after 3 months of storage (data shown in Figure S3). Hence, the powder form of the conjugates might provide a promising platform for clinical applications, due to the ease by which it can be stored, transported and re-suspended prior to use.

An important aspect of the PEO-*b*-(PPE-*g*-PTX) nanoparticle system is an ability to undergo hydrolytic degradation to release the PTX and allow it to perform its chemotherapeutic activity, while also eliminating the polymer nanoparticle structure. Aqueous solution-state hydrolysis studies were, therefore, conducted by observing breakdown of the polyphosphoester backbone by ^{31}P NMR spectroscopy as a function of time and pH, using the PEO-*b*-PPE block copolymer **3** as a model system, dissolved in D_2O at different pH

values (see Figure S4). At neutral pH, the polyphosphoester was fully stable over the entire period of measurement, >150 h. The rate and extent of hydrolysis increased with increasing pH. As the pH was reduced to acidic values, complications occurred with aggregation and precipitation events preventing accurate determination of the extent of hydrolysis, however, there was a general trend of increased hydrolysis, relative to neutral pH. A full study of the hydrolytic characteristics of these highly interesting polyphosphoester block copolymer nanoassemblies, as a function of composition and structure, is receiving further attention as a full, separate study. The hydrolytic release of PTX from PPE-PTX conjugates were measured by HPLC. However, only 5 % of PTX was released from PPE-PTX micelles after 4 days incubation in 20 mM acetate buffer at pH = 6.0. The lower release of PTX may be due to the inaccessibility of 2' PTX-ester in the hydrophobic core. To improve the release rate of PTX from PPE-PTX conjugates, next generations of PPE-PTX drug conjugates with acid-labile and redox-labile linkages are currently under development.

The PEO-*b*-(PPE-*g*-PTX) nanoparticle system (55 wt% PTX loading) was studied for its cytotoxic effect against several cancer cell lines. Both the Cremophor-EL/ethanol (1:1 *v/v*) and PEO-*b*-PPE polymers (control polymer **8**, see Figure S5 for the chemical structure) were not cytotoxic to the cells at the concentrations that were tested for the delivery of PTX (data not shown). The PTX conjugated onto the nanoparticles showed 8-to-63-fold lower cytotoxicity than the commercial PTX, depending on the sensitivity of the tested cell line to the drug (Table 1). The reduced cytotoxicity is explained by the time required for dissociation of the conjugated drug from the PEO-*b*-PPE backbone, followed by the physical release from the nanoparticles, in contrast to the drug that is physically loaded into the low molecular weight surfactant, Cremophor-EL. Lower cytotoxicities of PTX-polymeric drug conjugates, due to the slow *in vitro* release kinetics, have been previously reported in the literature. For instance, PGA-PTX conjugates exhibited 6-to-180-fold lower cytotoxicity than PTX, depending on the cell line utilized.[25] A contributing explanation could be the low cellular entry of the nanoparticles *versus* the possibility of the instantaneous release of PTX from the Cremophor-EL low molecular weight surfactant in the cell culture media, which can then passively diffuse into the cells and induce cytotoxicity.

To investigate the cell internalization of the PEO-*b*-(PPE-*g*-PTX) conjugates, a portion of the residual alkynyl groups were labeled with azido-functionalized fluorescein (Figures S6 and S7). The cellular uptake of the fluorescein-labeled PEO-*b*-(PPE-*g*-PTX) nanoparticles into OVCAR-3 cells and RAW 264.7 mouse macrophages was tested at different concentrations. After 5-h incubation (low cell viability was observed after longer incubation time.) and at PTX concentration of 15 μM, the nanoparticles could be visualized (green) in the cytoplasm of the RAW 264.7 cells surrounding the nucleus (blue) (Figure 3). In addition, morphological changes in the nucleus are observed, which may be due to apoptosis, induced by the released PTX (red arrows on Figure 3).[26] Lower concentrations on the same cell line (3 μM) or on OVCAR-3 (lower concentration (0.5 μM) is used due to the high sensitivity of this cell line to PTX, Table 1) could not observe the cellular uptake of the nanoparticles (Figure S8, supporting information). Even in the absence of visible nanoparticle uptake, nuclear fragmentation due to the released PTX was observed, however, to a lesser extent

(indicated also by the red arrows in Figure S8). Control-untreated cells or cells treated with PEO-*b*-PPE lacking PTX did not show any morphological changes in the nuclei.

In conclusion, we have developed a novel PEO-*b*-(PPE-*g*-PTX) drug conjugate system. Click chemistry was employed to attach bulky PTX molecules covalently and densely onto a select portion of the amphiphilic block copolymer backbone, and to label the resulting PEO-*b*-PPE-*g*-PTX system with fluorescein. In addition, residual alkynes provide possibilities of further post-chemical modifications (*e.g.* crosslinking, radio-labeling, decoration with targeting ligands), as opposed to the limited functionalizability of Taxol or Abraxane. Also in contrast to other promising PTX-based nanoparticle systems, the partitioning of separate PEO and PTX-functionalized PPE constituents within different regions along the block copolymer structure allows for placement of the components and their functions within different regions of the resulting nanoparticulate block copolymer micelle framework. The PEO-*b*-(PPE-*g*-PTX) achieved a PTX loading capacity as high as 65 wt% and, by balancing PTX loading capacity and polymer solubility, a water solubility at equivalent PTX concentration of 6.2 mg/mL was obtained (at 55 wt% PTX loading). Visualization of fluorescein-labeled PEO-*b*-(PPE-*g*-PTX) in cells by confocal fluorescence microscopy demonstrated the successful cellular internalization. Although the cell-killing activity of the covalently-conjugated PTX of PEO-*b*-(PPE-*g*-PTX) was reduced, relative to the physically-associated PTX of the Cremophor-EL and ethanol formulation, against several cancer cell lines, the lower cytotoxicity of the conjugates might be advantageous by providing increased safety for *in vivo* applications. For instance, the PEO-*b*-(PPE-*g*-PTX) nanoparticle micelle system could provide stability during blood circulation and allow release primarily after high accumulation in tumor tissues *via* the enhanced permeability and retention effect. The observation that accelerated hydrolytic degradation occurred for the polyphosphoester backbone at acidic pH is further promising for selective release in tumor cell environments, with a potential also for enzymatic catalysis. This PEO-*b*-(PPE-*g*-PTX) system provides a powerful platform for combinational therapy and bioimaging. Plans are underway for *in vivo* studies.

Supplementary Material

Refer to Web version on PubMed Central for supplementary material.

Acknowledgments

We gratefully acknowledge financial support from Covidien, Inc., the National Heart Lung and Blood Institute of the National Institutes of Health as a Program of Excellence in Nanotechnology (HHSN268201000046C) and the National Science Foundation under grant numbers DMR-0906815 and DMR-1105304. The Welch Foundation is gratefully acknowledged for support through the W. T. Doherty-Welch Chair in Chemistry, Grant No. A-0001. The transmission electron microscopy facilities at Washington University in St. Louis, Department of Otolaryngology, Research Center for Auditory and Visual Studies funded by NIH P30 DC004665 are gratefully acknowledged.

Notes and references

1. Rowinsky EK, Donehower RC. New. Engl. J. Med. 1995; 332:1004–1014. [PubMed: 7885406]
2. Spencer CM, Faulds D. Drugs. 1994; 48:794–847. [PubMed: 7530632]
3. Gelderblom H, Verweij J, Nooter K, Sparreboom A. Eur. J. Cancer. 2001; 37:1590–1598. [PubMed: 11527683]

4. Gradishar WJ. Expert Opin. Pharmaco. 2006; 7:1041–1053.
5. Singer JW. J. Control. Release. 2005; 109:120–126. [PubMed: 16297482]
6. Davis ME, Chen Z, Shin DM. Nat. Rev. Drug. Discov. 2008; 7:771–782. [PubMed: 18758474]
7. Brannon-Peppas L, Blanchette JO. Adv. Drug Deliver. Rev. 2004; 56:1649–1659.
8. Li C, Yu DF, Newman RA, Cabral F, Stephens LC, Hunter N, Milas L, Wallace S. Cancer Res. 1998; 58:2404–2409. [PubMed: 9622081]
9. Van S, Das SK, Wang XH, Feng ZL, Jin Y, Hou Z, Chen F, Pham A, Jiang N, Howell SB, Yu L. Int. J. Nanomed. 2010; 5:825–837.
10. Bonomi P. Expert. Rev. Anticanc. 2007; 7:415–422.
11. Li C, Wallace S. Adv. Drug Deliver. Rev. 2008; 60:886–898.
12. Zhang XQ, Xu XY, Lam R, Giljohann D, Ho D, Mirkin CA. ACS Nano. 2011; 5:6962–6970. [PubMed: 21812457]
13. Tong R, Cheng JJ. Angew Chem. Int. Edit. 2008; 47:4830–4834.
14. Zou J, Yu Y, Yu L, Li YK, Chen CK, Cheng C. J. Polym. Sci. Part A: Polym. Chem. 2012; 50:142–148.
15. Iwasaki Y, Yamaguchi E. Macromolecules. 2010; 43:2664–2666.
16. Du JZ, Du XJ, Mao CQ, Wang J. J. Am. Chem. Soc. 2011; 133:17560–17563. [PubMed: 21985458]
17. Elsabahy M, Wooley KL. Chem. Soc. Reviews. 2012; 41:2545–2561.
18. Zhang S, Li A, Zou J, Lin LY, Wooley KL. ACS Macro Lett. 2012; 1:328–333. [PubMed: 22866244]
19. Zhang S, Zou J, Zhang F, Elsabahy M, Felder SE, Zhu J, Pochan DJ, Wooley KL. J. Am. Chem. Soc. 2012; 134:18467–18474. [PubMed: 23092249]
20. Yu Y, Zou J, Yu L, Jo W, Li YK, Law WC, Cheng C. Macromolecules. 2011; 44:4793–4800.
21. Ernsting MJ, Tang WL, MacCallum N, Li SD. Bioconjugate Chem. 2011; 22:2474–2486.
22. Nakamura J, Nakajima N, Matsumura K, Hyon SH. Anticancer Res. 2010; 30:903–909. [PubMed: 20393013]
23. Johnson JA, Lu YY, Burts AO, Lim YH, Finn MG, Koberstein JT, Turro NJ, Tirrell DA, Grubbs RH. J. Am. Chem. Soc. 2011; 133:559–566. [PubMed: 21142161]
24. Iha RK, Wooley KL, Nystrom AM, Burke DJ, Kade MJ, Hawker CJ. Chem. Rev. 2009; 109:5620–5686. [PubMed: 19905010]
25. Yang D, Van S, Liu J, Wang J, Jiang XG, Wang YT, Yu L. Int. J. Nanomed. 2011; 6:2557–2566.
26. Ang ESM, Pavlos NJ, Chim SM, Feng HT, Scaife RM, Steer JH, Zheng MH, Xu J. J. of Cell. Biochem. 2012; 113:946–955. [PubMed: 22034016]

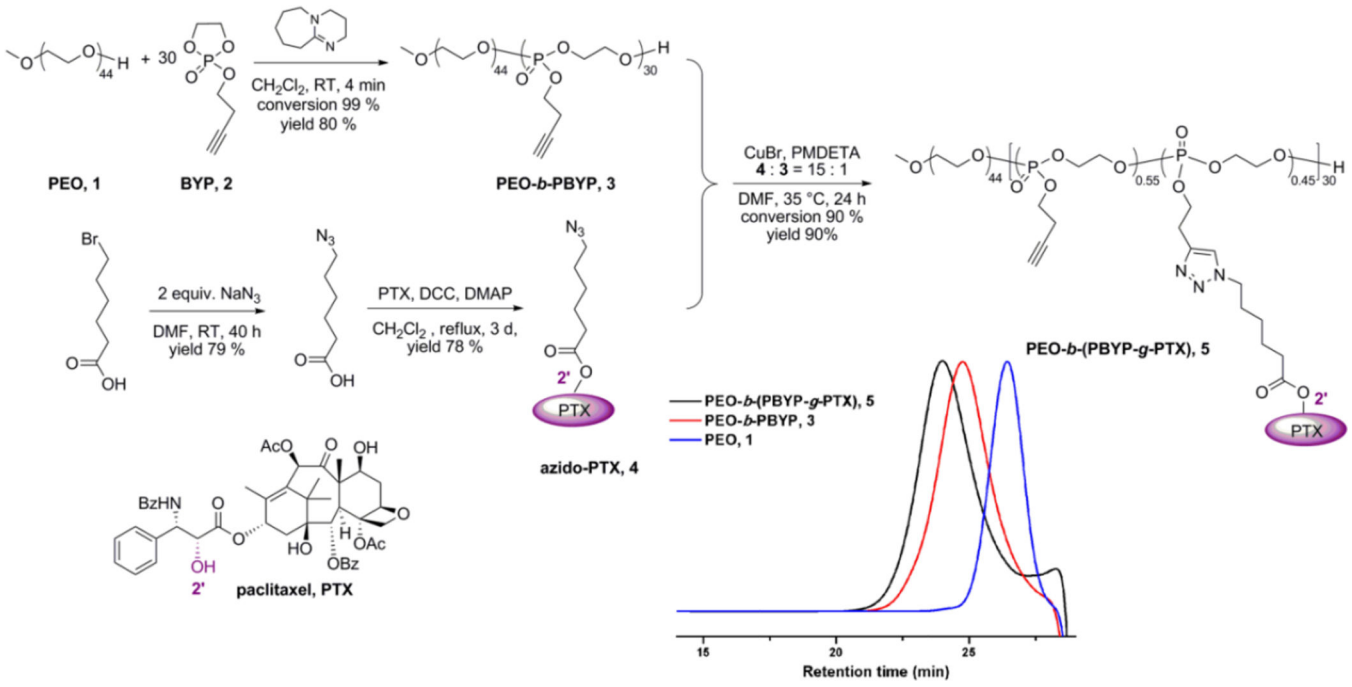

Fig. 1.

Schematic representation of the synthesis of PEO-*b*-(PTX-*g*-PBYP). GPC traces of PEO, PEO-*b*-PBYP and PEO-*b*-(PTX-*g*-PBYP) are inserted.

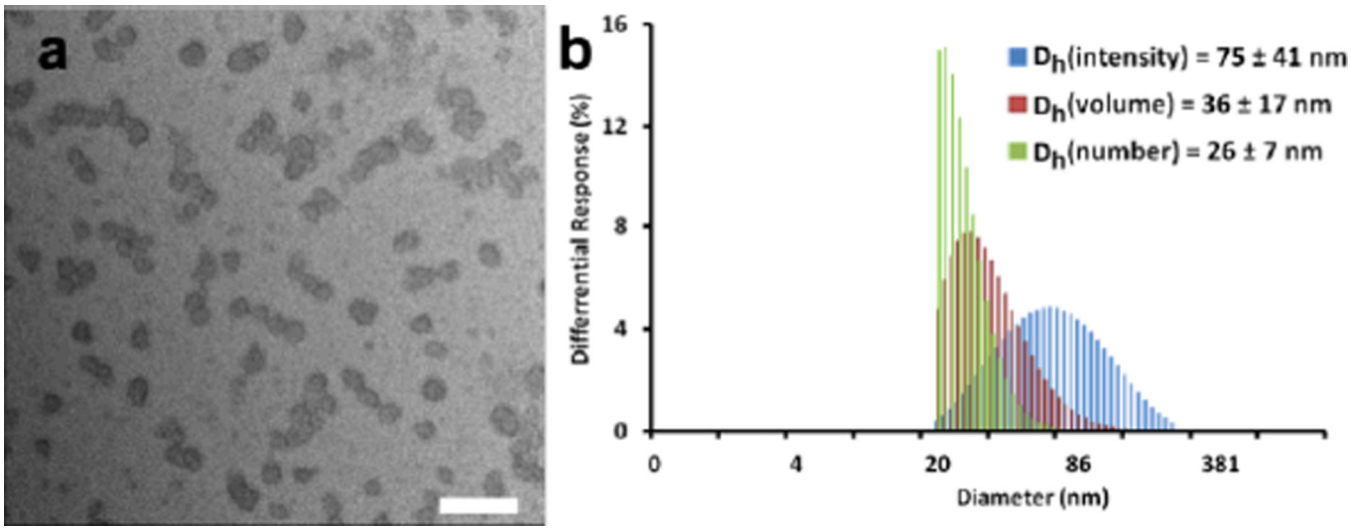

Fig. 2.

Micelles of **5** w/55 wt% PTX: a, TEM image, D_{av} = 24 ± 6 nm (scale bar: 100 nm); b, DLS in water.

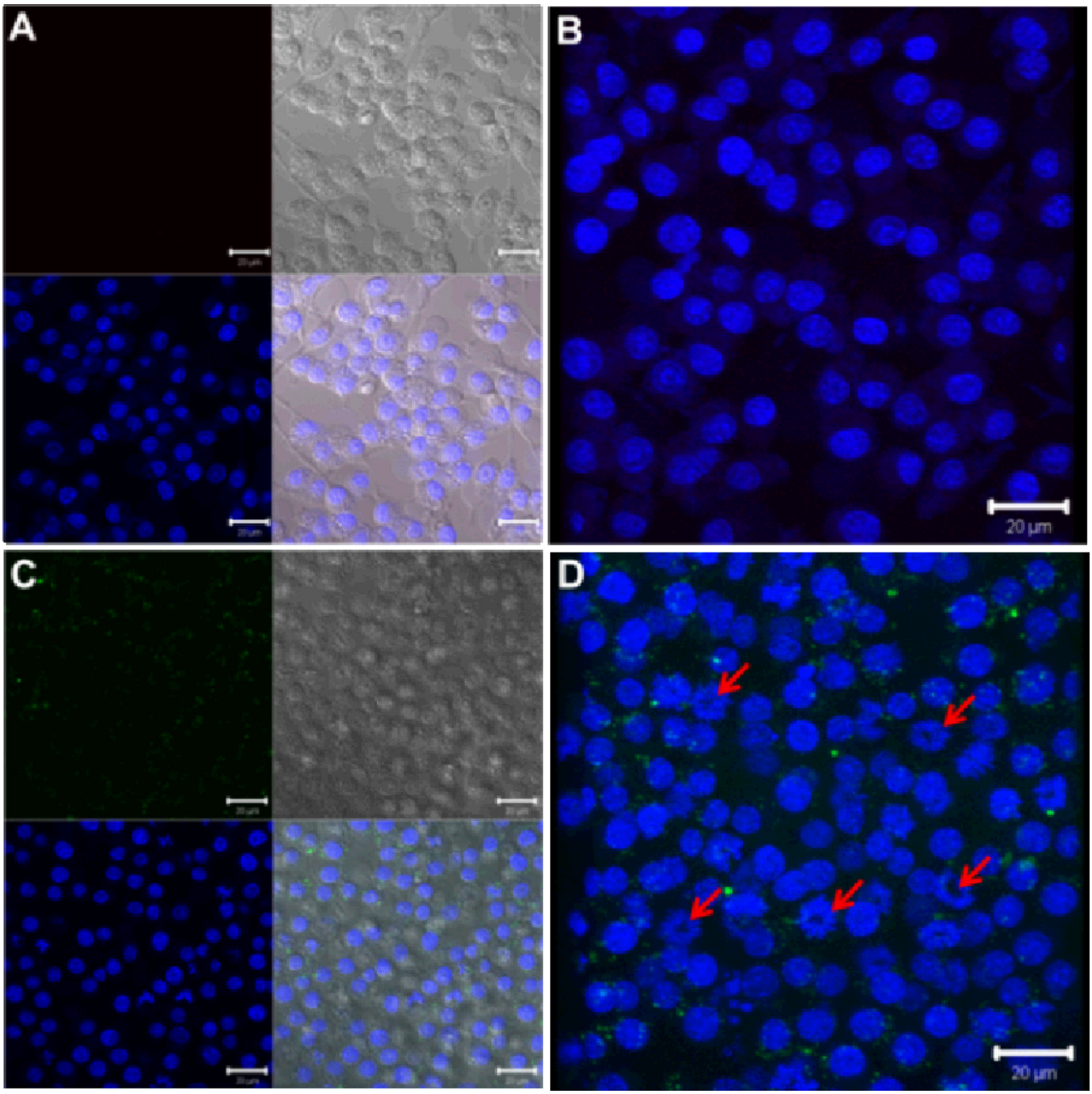

Fig. 3.

Laser scanning confocal microscopy analysis of the cellular uptake of fluorescein-labeled PPE-PTX nanoparticles (green panel) into RAW 264.7 mouse macrophages. Two- and three-dimensional images were collected for both the control-untreated cells (A and B) and the cells treated with the PTX-loaded nanoparticles (15 μM, C and D). The nuclei were stained with DRAQ5 nuclear stain (blue panel), whereas the fluorescein appears in green. The transmitted light-images and merged images are also indicated. The changes in the

nuclear morphology due to the treatment with the nanoparticles are demonstrated by the red arrows.

Table 1

Comparison of the IC_{50} values of PTX (as a Taxol®-mimicking formulation; Cremophor-EL and ethanol, 1:1 *v*/*v* with OVCAR-3 and RAW 264.7 cells, and free PTX with KB and A549 cell lines) and PTX conjugate, **5**, having 55 wt% PTX loading, incubated for 72 h.

Formulation	IC_{50} (μM)			
	OVCAR-3	RAW 264.7	KB cells	A549 cells
PTX	0.007	0.044	0.004	0.287
5	0.119	2.829	0.039	1.471